

# Neck formation and sub-barrier fusion of heavy-ion systems: $^{64}\text{Ni} + ^{100}\text{Mo}$ and $^{80}\text{Se} + ^{80}\text{Se}$

Dražen Vorkapić

*Institute of Nuclear Sciences "VINČA," YU-11101 Belgrade, Yugoslavia*

(Received 30 June 1993)

The fusion of  $^{64}\text{Ni} + ^{100}\text{Mo}$  and  $^{80}\text{Se} + ^{80}\text{Se}$  has been studied near and just below the Coulomb barrier. Fusion cross sections and average angular momenta have been calculated in a realistic neck formation fusion model based on barrier penetration, deformations, vibrations, and neck formation. The results agree well with the experimental data.

PACS number(s): 25.70.Jj

The measured cross section for the fusion of heavy ions at interacting energies near and below the Coulomb barrier can be strongly enhanced compared to one-dimensional barrier penetration calculations [1]. Theoretical studies have shown how the nuclear structure of the colliding nuclei produces these enhancements. A study of the fusion of  $^{16}\text{O}$  with samarium isotopes [2–6] illustrates the importance of nuclear deformations and zero-point vibrational motion in describing the behavior of the fusion cross sections. It has been shown that coupling to inelastic channels [7] or transfer channels [8] has the effect of splitting the Coulomb barrier and shifting some barriers to lower energy. Such effects resulted in enhanced sub-barrier fusion cross sections, thus improving the fit to the data.

Experimental investigations of the angular momentum distribution leading to fusion have provided important information that is complementary to the study of cross sections. Information on the angular momenta involved in sub-barrier fusion have been obtained with three different techniques [9]:  $\gamma$ -ray multiplicity, fission fragment angular distributions, and measurement of isomer ratios. These measurements have revealed broadening of the spin distributions expected from coupled-channel calculations [7,8,10] (coupling to collective excitations and transfer channels). The average angular momenta  $\langle l \rangle$  and the associated cross sections  $\sigma_{\text{fus}}$  for 14 systems have been analyzed [9] with coupled-channel models. Good agreement was found between the theory and data with the exception of the more symmetric systems ( $^{64}\text{Ni} + ^{100}\text{Mo}$  [11] and  $^{80}\text{Se} + ^{80}\text{Se}$  [9,12–14,24]). In the present paper we consider this disagreement, studying the effect of neck formation on sub-barrier fusion cross sections.

The coupled-channel model underestimated the fusion cross section for  $^{64}\text{Ni} + ^{100}\text{Mo}$  [11] at sub-barrier energies. Satisfactory agreement was obtained [11] with all the strengths of the  $\beta_\lambda$  from the literature multiplied by 1.5. Even with this large increase of parameters, average angular momenta  $\langle l \rangle$  and  $\langle l^2 \rangle$  were underestimated at sub-barrier energies.

Udagawa, Kim, and Tamura [15] have been successful in fitting fusion cross section  $\sigma_{\text{fus}}$  and average angular momentum  $\langle l \rangle$  by separating the absorptive potentials into a fusion part and direct reaction part by a cutoff at some particular reduced radius adjusted to fit  $\sigma_{\text{fus}}$ . This

radius turns out to be rather large  $r_F \simeq 1.4\text{--}1.5$  fm, which means that fusion occurs outside the barrier. The model of Udagawa, Kim, and Tamura [15] does not provide information concerning the physical phenomena that might be responsible for fusion at such large distances.

We will formulate a neck formation fusion model (NFFM) for two deformed or vibrational nuclei. The assumption of the NFFM is that the neck forms outside the unperturbed barrier leading to fusion. The large  $r_F$  in the Udagawa model [15] has been explained by neck formation. Using the classical dynamical model Aguiar, Canto, and Donangelo [16] have pointed out that the formation of the neck may explain the lowering of the barrier. Later Iwamoto and Harada [17] have calculated sub-barrier fusion cross sections for symmetric systems, based on the idea of neck formation. Stelson *et al.* [18] have pointed out that the barrier for neutron transfer vanishes at distances typically 1.5 fm beyond the typical barrier distance. The presence of neutrons in the region between the nuclei could promote neck formation, which provides a force strong enough to overcome the Coulomb force.

The two nuclei are randomly oriented. The angles between the internuclear separation axis and symmetry axis of both the deformed projectile and target nucleus are denoted by  $\Theta_1$  and  $\Theta_2$ , respectively. The shape of both nuclei is frozen during the collision. For every orientation  $(\Theta_1, \Theta_2)$  we use the Hill-Wheeler formula [19] for the penetration factor  $P_l(E, \Theta_1, \Theta_2)$ , which represents the probability that a given partial wave  $l$  in the entrance channel leads to fusion. We approximate the various effective interacting potentials around their relative maxima by inverted parabolas of height  $V_l(\Theta_1, \Theta_2)$  and frequency  $\omega_l(\Theta_1, \Theta_2)$ . For a parabolic barrier the penetration coefficients  $P_l(E, \Theta_1, \Theta_2)$  are given exactly by the Hill-Wheeler formula [19]

$$P_l(E, \Theta_1, \Theta_2) = 1 / (1 + e^{2\pi(V_l - E)/\hbar\omega_l}) , \quad (1)$$

which is quantum mechanically correct for energies  $E$  both above and below  $V_l$ . The frequency  $\omega_l$  depends on both the barrier curvature and the inertia parameter  $\mu$

$$\omega_l(\Theta_1, \Theta_2) = \{ (1/\mu) [(\partial^2/\partial r^2) V_{\text{eff}}(l, r)]_{R_l} \} , \quad (2a)$$

where  $R_l$  is given by

$$(dV_{\text{eff}}/dr)_{r_i} = 0. \quad (2b)$$

The effective potential for the radial motion of the two nuclei is

$$V_{\text{eff}}(r) = V_{\text{Coul}}(r, \Theta_1, \Theta_2) + V_{\text{nucl}}(r, \Theta_1, \Theta_2) + l(l+1)\hbar^2/2\mu r^2. \quad (3)$$

The first term is the Coulomb interaction containing monopole, quadrupole, and octupole terms. The second term is the nuclear interaction. In some systems we use the nucleus-nucleus proximity potential [20]

$$V_{\text{prox}} = 4\pi\gamma Rb\Phi_{\text{prox}}[(r - C_1 - C_2)/b], \quad (4a)$$

$$R = C_1 C_2 / (C_1 + C_2), \quad (4b)$$

$$C_i = R_i - b^2/R_i,$$

$$R_i = 1.28 A_i^{1/3} - 0.76 + 0.8 A_i^{-1/3}.$$

Here  $\gamma$  is the surface energy coefficient,  $b$  is the diffuseness of the nuclear surface estimated as  $b = 1$  fm,  $r$  is the distance between the centers of the interacting nuclei, and  $\Phi_{\text{prox}}$  is the proximity function tabulated by Blocki *et al.* [21]. The radius of a projectile or target de-

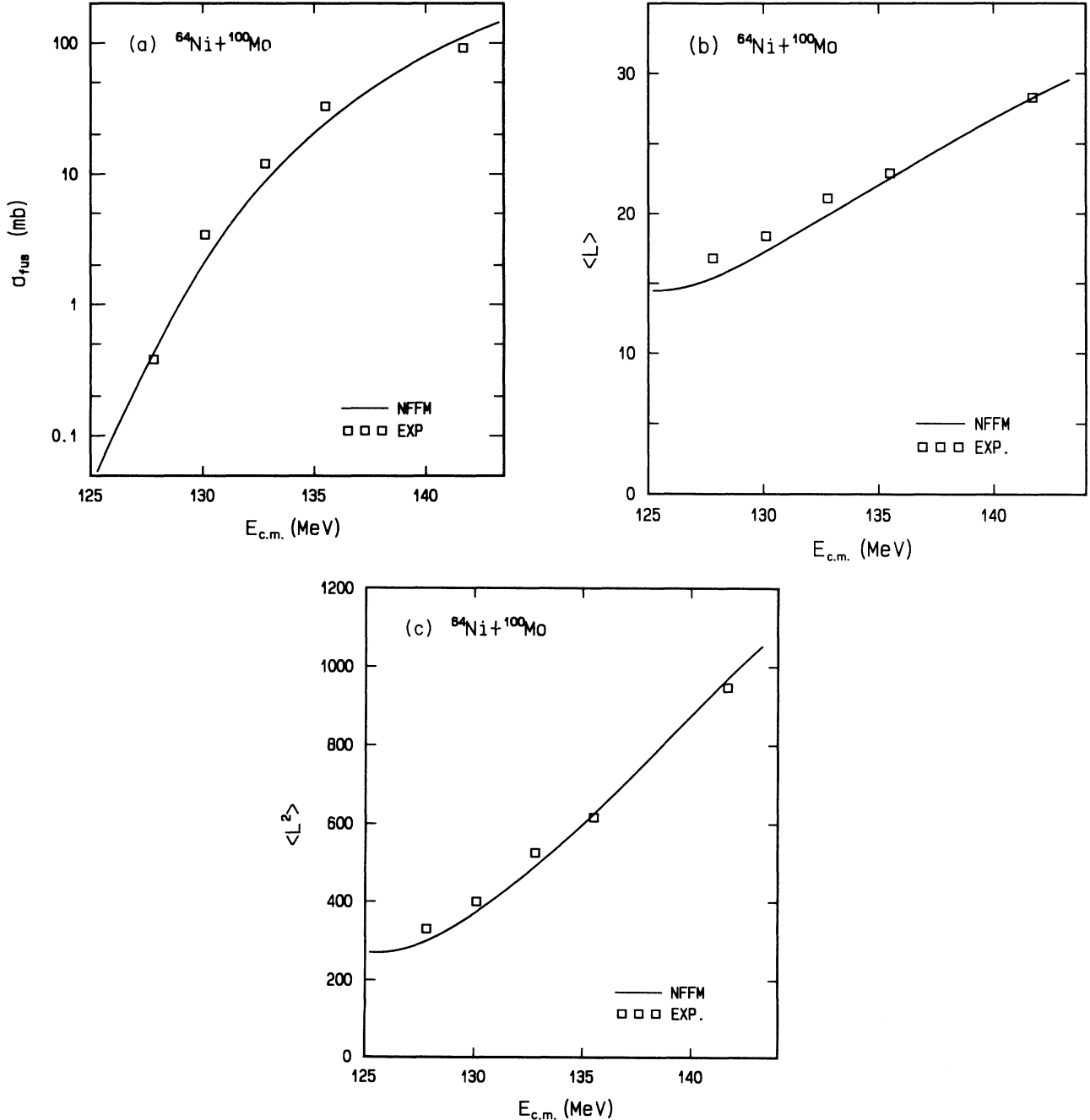


FIG. 1. Predicted and experimental (a) fusion cross sections, (b) average angular momenta, and (c) mean square angular momenta for the fusion of  $^{64}\text{Ni} + ^{100}\text{Mo}$ . The squares are the experimental data. The theoretical predictions are shown by the solid lines.

depends on the angle of orientation  $\Theta_i$  through the equation

$$C_i(\Theta_i) = C_i \left[ 1 + \sum \beta_\lambda Y_\lambda(\Theta_i) \right], \quad (5)$$

where  $\beta_\lambda$  is deformation parameter. Here in the NFFM we introduce a cylindrical neck between the two nuclei, and the nuclear interaction energy is given by [22]

$$V_{\text{neck}} = 2\pi\gamma c(d_{\text{eff}} - c) + 4\pi\gamma R b \Phi_{\text{prox}}(d/b) \exp(-c^2/2Rb), \quad (6a)$$

$$d_{\text{eff}} = d - s_{\text{crit}} [1 - (c/2R)], \quad (6b)$$

$$d = s + c^2/2R, \quad (6c)$$

$$s = r - C_1 - C_2. \quad (6d)$$

The first term is an extra surface energy associated with the cylindrical neck of radius  $c$ ,  $d_{\text{eff}}$  is the effective neck length, and  $s_{\text{crit}} = 1.78$  fm is the critical separation at which the neck first forms. The neck dynamics is described by

$$c = s_{\text{crit}} - s. \quad (7)$$

The overall fusion cross section corresponds to an average taken over all possible orientations of both nuclei

$$\sigma_{\text{fus}} = \sum \sigma_l = \sum (2l+1) \langle P_l(E, \Theta_1, \Theta_2) \rangle. \quad (8)$$

The average angular momentum and mean square angular momentum are given by

$$\langle l \rangle = \sum l \sigma_l / \sigma_{\text{fus}}, \quad (9a)$$

$$\langle l^2 \rangle = \sum l^2 \sigma_l / \sigma_{\text{fus}}. \quad (9b)$$

The rotational nuclei are characterized by permanent deformation. In the case of vibrational nuclei the surface fluctuates as a result of zero-point motion [6] and we have effective deformation parameters given by

$$\beta_\lambda = [1/Z_2(\lambda+3)] \{4\pi(2\lambda+1)[B(E\lambda)/B_W(E\lambda)]\}^{1/2}, \quad (10)$$

where  $B_W(E\lambda)$  is the Weiskopf units and  $Z_2$  is the charge of the target nucleus. For high-lying vibrations, the vibrational enhancements are increasingly damped out, and effective deformation parameters will be less than  $\beta_\lambda$  from (10). For very high vibrations the adiabatic approximation is no longer valid. The neck formation potential in the NFFM is lowered compared to unperturbed potentials, the radius corresponding to the maximum of the barrier is shifted to a larger value and there is an increase in  $\hbar\omega_l$  (5–6 MeV). It should be emphasized that for the case of vibrational nuclei the increase in phonon energy will amplify the damping of the vibrational enhancement.

By means of the code SFUS2 [23] (which treats neck formation fusion) we could calculate the sub-barrier fusion of  $^{64}\text{Ni} + ^{100}\text{Mo}$ . The shapes were taken to be described by effective deformation parameters  $\beta_2 = 0.23$  and  $0.15$  for  $^{100}\text{Mo}$  and  $^{64}\text{Ni}$ , respectively. The predicted and measured fusion cross sections  $\sigma_{\text{fus}}$ , average angular momenta  $\langle l \rangle$ , and mean square angular momenta  $\langle l^2 \rangle$  are com-

pared in Fig. 1. The curves in Fig. 1 are NFFM calculations carried out with the program SFUS2 and they reproduce reasonably well the experimental results. It should be noted that such agreement could not be accidental for all three figures [Figs. 1(a), 1(b), and 1(c)]. At low energies in the NFFM the average value of the angular momentum becomes a constant, which is large compared to coupled-channel models.

The second case is the symmetric system  $^{80}\text{Se} + ^{80}\text{Se}$  [9,12–14,24]. Dasso, Garrett, and Landowne [14] have been able to reproduce the general feature of the multipli-

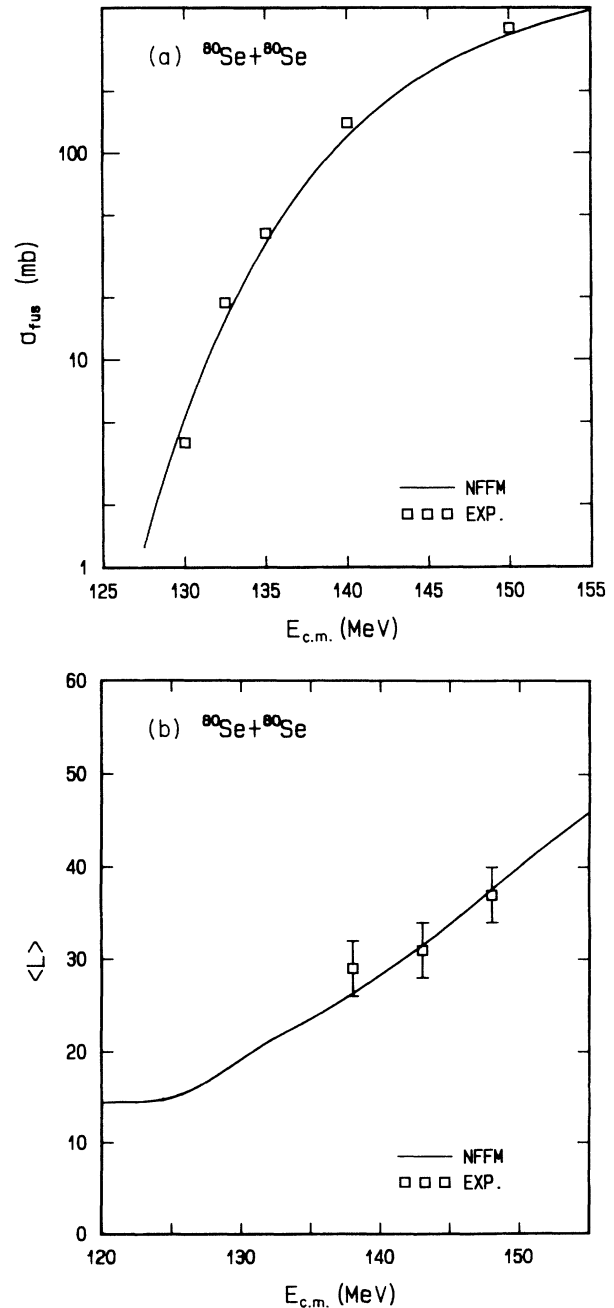


FIG. 2. Theoretically predicted and experimental (a) fusion cross sections and (b) average angular momenta for the fusion of  $^{80}\text{Se} + ^{80}\text{Se}$ .

city distribution from Ref. [12], but in that process the relative fusion cross section was overestimated by factors of 2–3 at the lowest energies. We must be careful with angular momenta in Ref. [12], since angular momenta for low energies were measured only for the  $2n$  channel. For the  $^{80}\text{Se}+^{80}\text{Se}$  system the angular momenta for the  $3n$  channel is dominant (but not measured) and therefore total average angular momenta were not given by experiment in Ref. [12]. Average angular momenta have been measured in the fusion reaction  $^{80}\text{Se}+^{80}\text{Se}$  at near-barrier energies by Haas *et al.* [13]. The results were interpreted in terms of ground-state zero-point vibrations. NFFM calculations were carried out for  $^{80}\text{Se}$  shapes with an effective deformation parameter  $\beta_2=0.19$ . We show in Fig. 2(a) the predicted and measured fusion cross sections. The agreement is good. Average angular momenta  $\langle l \rangle$  have been measured with big uncertainties and not at sub-barrier energies. Although theoretical results can reproduce all three experimental points [Fig. 2(b)], we

must be careful because these results were also interpreted in terms of zero-point vibration and coupled-channel calculations. But fusion cross sections for sub-barrier energies were explained only in the NFFM calculation. It should be noted that the constant average angular momentum at low bombarding energies has been obtained in NFFM calculations [Fig. 2(b)]. The predicted constant ( $l \simeq 15$ ) is large compared to the prediction from Ref. [24] ( $l \simeq 10$ ).

The advantage of our model is the small number of parameters. The NFFM is described by only two effective deformation parameters. The NFFM was applied to heavy systems near symmetry. These results have been explained by the introduction of neck formation. Additional work is required to elucidate the importance of neck formation in systems far from symmetry. Work in this direction would benefit from additional measurements of angular momenta at sub-barrier energies.

- 
- [1] M. Beckerman, *Phys. Rep. B* **129**, 145 (1985).
  - [2] S. Gil, R. Vandenbosch, A. Charlop, A. Garcia, D. D. Leach, S. J. Luke, and S. Kailas, *Phys. Rev. C* **43**, 701 (1991).
  - [3] S. Gil, R. Vandenbosch, A. J. Lazzarini, D.-K. Lock, and A. Ray, *Phys. Rev. C* **31**, 1752 (1985).
  - [4] R. G. Stokstad and E. E. Gross, *Phys. Rev. C* **23**, 281 (1981).
  - [5] L. C. Vaz, J. M. Alexander, and R. G. Satchler, *Phys. Rep.* **69**, 373 (1981).
  - [6] H. Esbensen, *Nucl. Phys.* **A352**, 147 (1981).
  - [7] C. D. Dasso, S. Landowne, and A. Winther, *Nucl. Phys.* **A405**, 381 (1983).
  - [8] R. A. Broglia, C. H. Dasso, S. Landowne, and G. Pollaro, *Phys. Lett.* **133B**, 34 (1983).
  - [9] D. E. DiGregorio and R. G. Stokstad, *Phys. Rev. C* **43**, 265 (1991).
  - [10] C. H. Dasso and S. Landowne, *Phys. Lett. B* **183**, 141 (1987).
  - [11] M. L. Halbert, J. R. Beene, D. C. Hemsley, K. Honkanen, T. M. Semkow, V. Abenante, D. G. Sarantites, and Z. Li, *Phys. Rev. C* **40**, 2558 (1989).
  - [12] P. J. Nolan, D. J. G. Love, A. Kirwan, D. J. Unwin, A. H. Nelson, P. J. Twin, and J. D. Garrett, *Phys. Rev. Lett.* **54**, 2211 (1985).
  - [13] B. Hass, G. Duchene, F. A. Beck, T. Byrski, C. Gehringer, J. C. Merdinger, A. Nourredine, V. Rauch, J. P. Vivien, J. Barrette, S. Tobbeche, E. Bozek, J. Styczen, J. Keinonen, J. Dudek, and W. Nazarewicz, *Phys. Rev. Lett.* **54**, 398 (1985).
  - [14] C. H. Dasso, J. D. Garrett, and S. Landowne, *Phys. Lett.* **161B**, 36 (1985).
  - [15] T. Udagawa, B. T. Kim, and T. Tamura, *Phys. Rev. C* **32**, 124 (1985).
  - [16] C. E. Aguiar, L. F. Canto, and R. Donangelo, *Phys. Rev. C* **31**, 1969 (1985).
  - [17] A. Iwamoto and K. Harada, *Z. Phys. A* **326**, 201 (1987).
  - [18] P. H. Stelson, H. J. Kim, M. Beckerman, D. Shapira, and R. L. Robinson, *Phys. Rev. C* **41**, 1584 (1990).
  - [19] D. L. Hill and J. A. Wheeler, *Phys. Rev.* **89**, 1102 (1953).
  - [20] B. B. Back, R. R. Betts, J. E. Gindler, R. D. Wilkins, S. Saini, M. B. Tsang, C. K. Gelbke, W. G. Lynch, M. A. McMahan, and P. P. Baisden, *Phys. Rev. C* **32**, 195 (1985).
  - [21] J. Blocki, J. Randrup, W. J. Swiatecki, and C. F. Tsang, *Ann. Phys.* **105**, 427 (1977).
  - [22] J. Randrup, *Nucl. Phys.* **A383**, 468 (1982).
  - [23] D. Vorkapić, computer code SFUS2 (unpublished).
  - [24] C. H. Dasso and S. Landowne, *Phys. Rev. C* **32**, 1094 (1985).